**Proceedings of the ASME 2012 International Design Engineering Technical Conferences & Computers and Information in Engineering Conference**
**IDETC/CIE 2012**
**August 12-15, 2012, Chicago, IL, USA**

**DETC2012-71082**

# PRELIMINARY VALIDATION OF COMPOSITE MATERIAL CONSTITUTIVE CHARACTERIZATION

**John G. Michopoulos**
Computational Multiphysics Systems Lab.
Center of Computational Material Science
Naval Research Laboratory
Washington DC 20375, USA

**Athanasios Iliopoulos**
Computational Materials Science Center
George Mason University, Fairfax VA 22030, USA
resident at Center of Computational Material Science
Naval Research Laboratory
Washington DC 20375, USA

**John C. Hermanson**
Wood Based Materials & Structures
Forest Products Laboratory
USDA Forest Service
Madison, WI, USA

**Adrian C. Orifici**
School of Aerospace, Mechanical and Manufacturing Engineering
RMIT University
Melbourne, Victoria, 3001, Australia

**Rodney S. Thomson**
Cooperative Research Centre for
Advanced Composite Structures Limited
Fishermans Bend, Victoria, 3207, Australia

## ABSTRACT

*This paper is describing the preliminary results of an effort to validate a methodology developed for composite material constitutive characterization. This methodology involves using massive amounts of data produced from multiaxially tested coupons via a 6-DoF robotic system called NRL66.3 developed at the Naval Research Laboratory. The testing is followed by the employment of energy based design optimization principles to solve the inverse problem that determines the unknown parameters of the constitutive model under consideration. In order to validate identified constitutive models, finite element simulations using these models were exercised for three distinct specimen geometries. The first geometry was that of the characterization coupon under multiaxial loading. The second was that of open hole specimens in tension. The final one was that of stiffened panel substructures under tension. Actual experimental data from testing all these specimens were collected by the use of load cells, full field displacement and strain methods and strain gauges. Finally, the theoretical predictions were compared with the experimental ones in terms of strain field distributions and load-strain responses. The comparisons demonstrated excellent predictability of the determined constitutive responses with the predictions always within the error band of the methods used to collect the experimental data.*

## INTRODUCTION

The present work has been motivated by the need to confirm that data-driven constitutive characterization methodologies are indeed capable of predicting the behavior of composite materials used to make structures in shapes similar or different than those used for the characterization experiments. Essential to this confirmation is the activity of validating the constitutive models identified by our proposed characterization methodologies.

This paper is a natural follow-up of our previous work [1, 2] on methodologies for the identification of material constants associated with constitutive models encapsulated in energy density formalisms, by solving inverse problems utilizing massive amounts of experimental data collected from multiaxially loaded coupons. This work complements the first industrial rate completion of 1152 composite coupon tests for characterization purposes as reported in a companion paper [3] also submitted to this conference.

Our collaborative effort focuses on designing, planning and executing tests of composite material specimens and collecting kinematic and resulting strain field data to be used for the purpose of comparing them with theoretical predictions produced by using the identified constitutive behaviors within finite element analysis (FEA) that simulate the behavior of these specimens.

In this paper, we describe the validation methodology that we followed and its application for three distinct types of specimens. The first type of specimens involves coupon specimens used for the characterization process tested with the NRL66.3 multiaxial system. However, the associated experimental data collected were not used for the constitutive characterization process. The second type of specimens are open hole specimens tested in tension. The final type of specimens are stiffened panel specimens also tested in tension. For each one of these specimens, full 3D FEA analyses were implemented by using the characterized constitutive models. The FEA results are compared with the experimental data collected. All comparisons are discussed and finally conclusions are presented.

## CHARACTERIZATION AND VALIDATION

The methodology followed for characterization has been described in detail elsewhere [1, 2] and the first industrialized method of experiments has been completed and described in a companion paper in this conference [3]. Due to space limitations we are not going to describe an overview of these methodologies here again and we advise the reader to consult the above referenced publications.

However, we have to underline that we used two energy density based constitutive models. One is based on the small strain formulation (SSF) and another is based on the finite strain formulation (FSF). For the case of the SSF approach, the corresponding anisotropic elastic constants fully describing the elastic behavior of the AS4/3501-6 composite are presented in table 1 in units ap-

**TABLE 1**: IDENTIFIED AS4/3501-6 CARBON/EPOXY PROPERTIES FOR SSF

| Property | expressions | Value | Units |
|---|---|---|---|
| $E_{xx}$ | $E_1$ | 125000 | $N/mm^2$ |
| $E_{yy}$ | $E_2$ | 10800 | $N/mm^2$ |
| $E_{zz}$ | $E_2$ | 10800 | $N/mm^2$ |
| $\nu_{xy}$ | $\nu_{12}$ | 0.270 | |
| $\nu_{yz}$ | $\nu_{23}$ | 0.32 | |
| $\nu_{xz}$ | $\nu_{12}$ | 0.270 | |
| $G_{xy}$ | $G_{12}$ | 7960 | $N/mm^2$ |
| $G_{yz}$ | $\frac{E_{yy}}{2(1+\nu_{yz})}$ | 4039 | $N/mm^2$ |
| $G_{xz}$ | $G_{12}$ | 7960 | $N/mm^2$ |

**TABLE 2**: IDENTIFIED AS4/3501-6 CARBON/EPOXY PROPERTIES FOR FSF

| Property | Value |
|---|---|
| $d$ | 0.00007012 |
| $a_1$ | 1611 |
| $b_1$ | 713 |
| $c_2$ | 29212 |
| $e_2$ | -458.7 |
| $d_a^\infty$ | 0.1 |
| $\eta_a$ | 1.2 |

propriate for using with the ANSYS FEA package. Similarly, the constants identified for the FSF are and used in the FEA analysis are shown in table 2

To demonstrate the validity of the constitutive models determined by our approach, we incorporated the identified SSF and FSF constitutive and 3D geometrical specimen models into ANSYS for analysis.

The validation consisted of comparing the experimental strain to those derived from the corresponding FEA analyses. For those validations tests where strain gauges were used to moni-

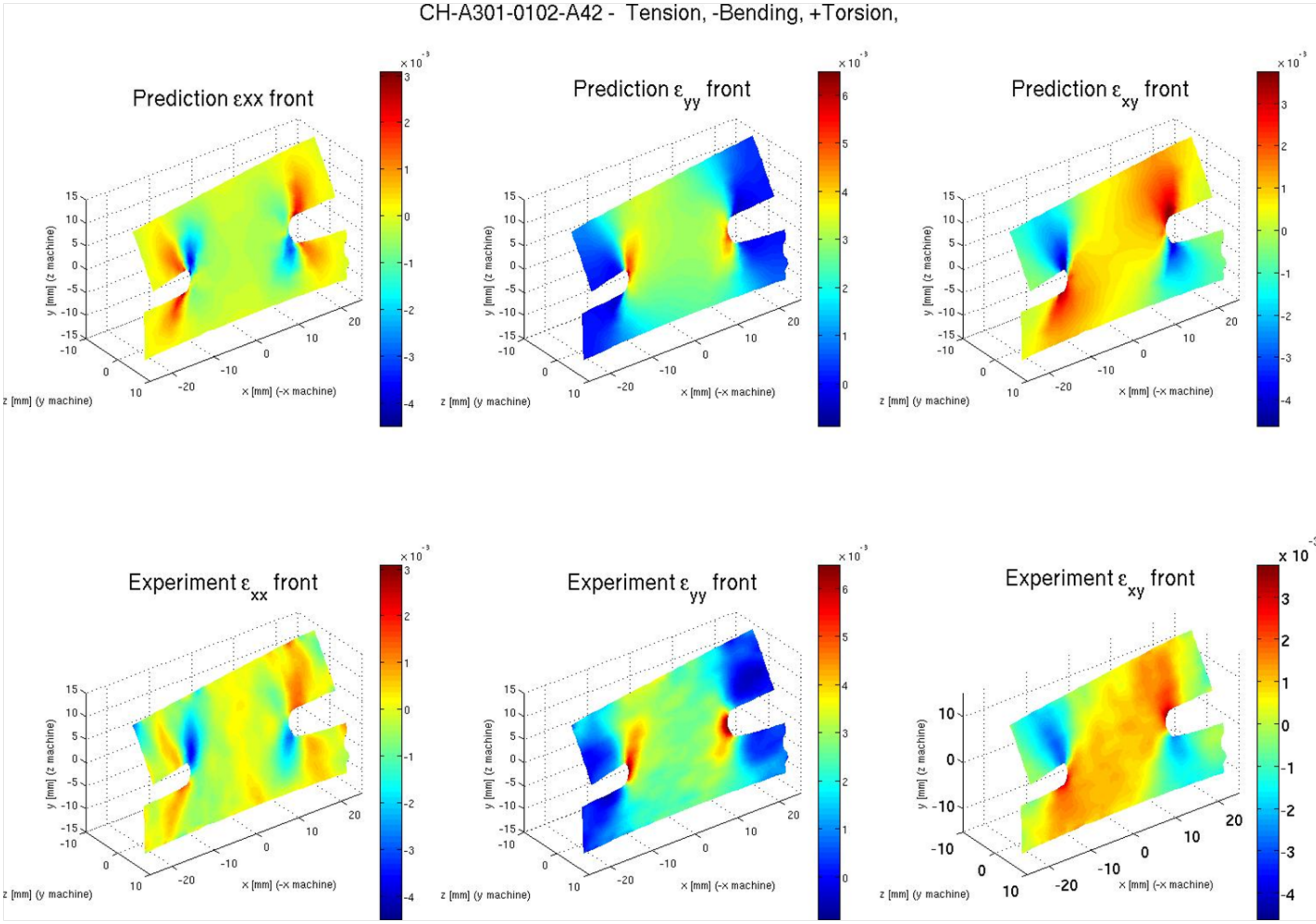


**FIGURE 1**: PREDICTED (TOP ROW) VS. EXPERIMENTAL (BOTTOM ROW) STRAIN COMPONENT FIELDS DISTRIBUTIONS FOR A CHARACTERIZATION COUPON UNDER COMBINED TENSION, BENDING AND TORSION LOADING

tor evolution of strain, we compare load vs. strain curves. For those tests where RemDiS-2D or RemDiS-3D has been used to monitor displacement and strain evolutions, we compare load vs. strain curves fields.

The Finite Element Analysis (FEA) was implemented in the ANSYS [4]. The main aim of the verification comparison in this work was to develop as a detailed model as possible and hence a full 3D model was constructed and analysis was performed. The full 3D model is capable of modeling through thickness characteristics and higher order behavior of the energy, stress and strain fields, that is not available with any of the laminate theories, even the higher order ones.

## VALIDATION WITH CHARACTERIZATION SPECIMENS

The first validation simulation were performed for the typical double notched characterization specimen described elsewhere [3], but for loading paths that were not used for determining the constitutive model itself.

For the sake of brevity we will not describe here the details of the geometry and layup configuration nor the details of the full 3D FEA model used for the predictions of the behavior of the characterization specimens

As a representative validation prediction we are presenting the results for two loading paths. It is important to emphasize that the experimental data obtained from the associated tests were not used in determining the constitutive constants (material parameters) that are fixing the associated constitutive model.

Figure 1 shows the three strain field distributions at the same loading step of a load path that involves tension, out of plane

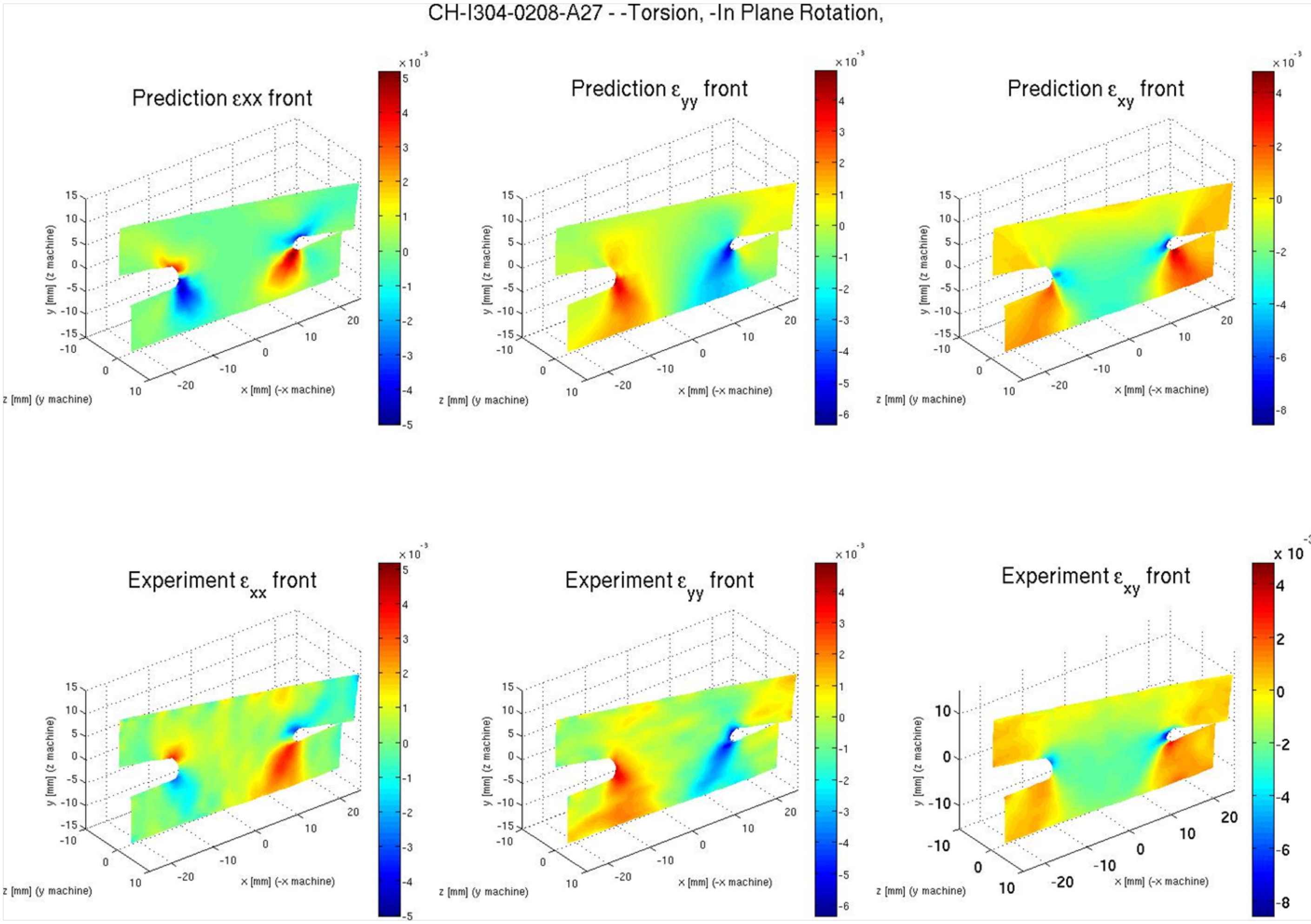


**FIGURE 2**: PREDICTED (TOP ROW) VS. EXPERIMENTAL (BOTTOM ROW) STRAIN COMPONENT FIELDS DISTRIBUTIONS FOR A CHARACTERIZATION COUPON UNDER COMBINED IN-PLANE ROTATION AND TORSION LOADING

bending and torsion about the longitudinal axis.

Figure 2 shows the three strain field distributions at the same loading step of a load path that involves tension, in plane rotation and torsion about the longitudinal axis.

All predicted strain field distributions for both of these cases, show that the predicted values are within 4% error of the experimental ones. This is well within the error of the RemDiS-3D experimental method.

## VALIDATION WITH OPEN HOLE SPECIMENS

The second set of validation simulations was performed for open hole specimens under tension. The specimens used for the validation tests were manufactured from the same base material used to construct the characterization specimens but in different layup. This material was AS4/3501-6 carbon/epoxy unidirectional prepreg, with nominal ply thickness of 0.13 mm. The generic specimen is depicted schematically in Fig. 3(a). The geometric particulars in table 3. A marked specimen used for the experiments is shown in Fig. 3(b). On the unmarked side of the specimens, strain-gauges were attached as shown in Fig. 3(a), designated as SG:Far for the one located far away from the hole and SG:Hole for the one located next to the hole.

The tests were conducted by CRC-ACS at the Defense Science and Technology Organization (DSTO), Melbourne, Australia. with the aid of a 250 kN Instron hydraulic test machine. The specimen was loaded in tension quasi-statically until ultimate failure.

The camera used for the full field measurements for the use of MRGM [5–10] and the ReMDiS-2D package [11], was a Canon eos 400D D-SLR.

The open hole specimen model consisted of 24 layers of

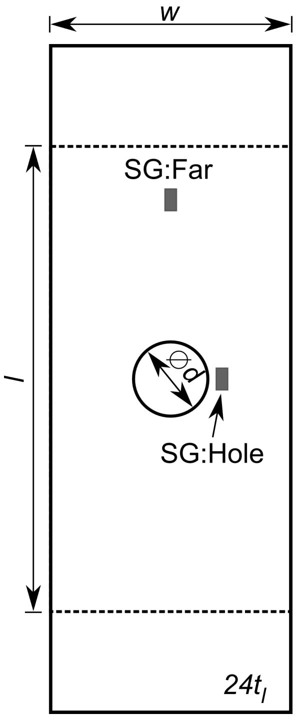


(a) Specimen geometry

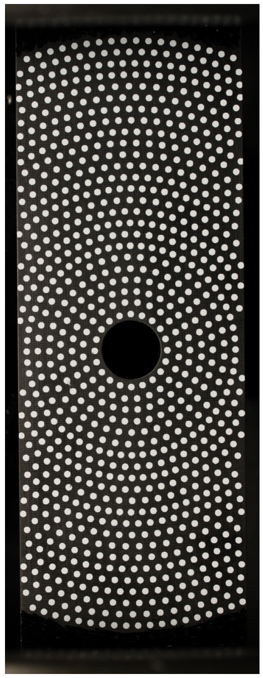

(b) Image of marked specimen

**FIGURE 3**: SPECIMEN GEOMETRY

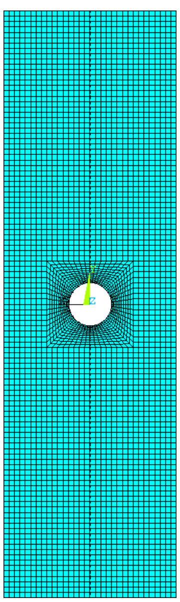

(a) Plan view

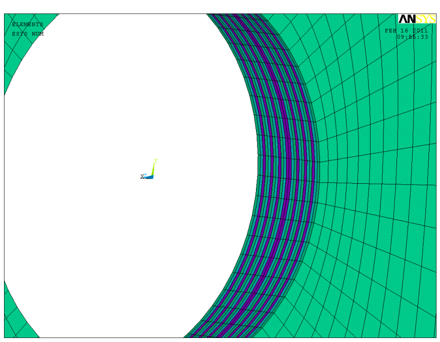

(b) Hole detail and colored element coordinate system

**FIGURE 4**: FINITE ELEMENT GEOMETRY

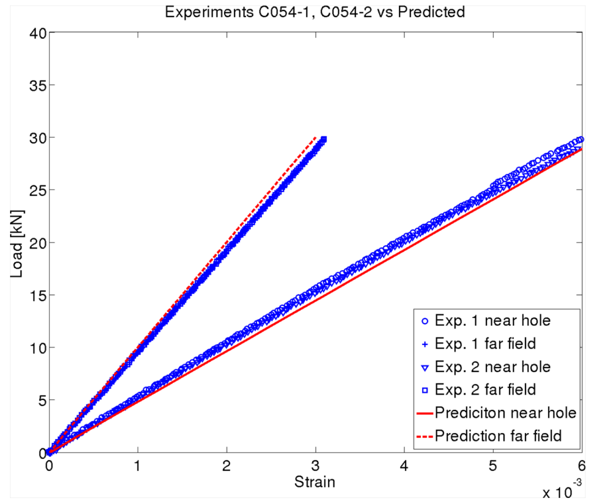


(a) 0.5 inch hole

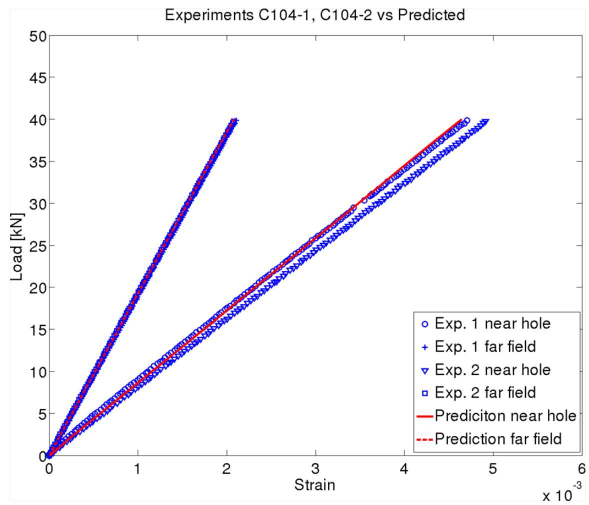


(b) 1 inch hole

**FIGURE 5**: OPEN HOLE SPECIMEN LOAD VS. STRAIN FOR THE SSF

**TABLE 3**: SPECIMEN GEOMETRY SPECIFICATION

| Parameter | Value | Units |
|---|---|---|
| Width $w$ | 50 | *mm* |
| Free Length $l$ | 170 | *mm* |
| Hole Diameter $d$ | 12.5 | *mm* |
| Ply Thickness $t_l$ | 0.13 | *mm* |
| Layup Type | $[-45^o, 0^o, 45^o]_{4S}$ | |

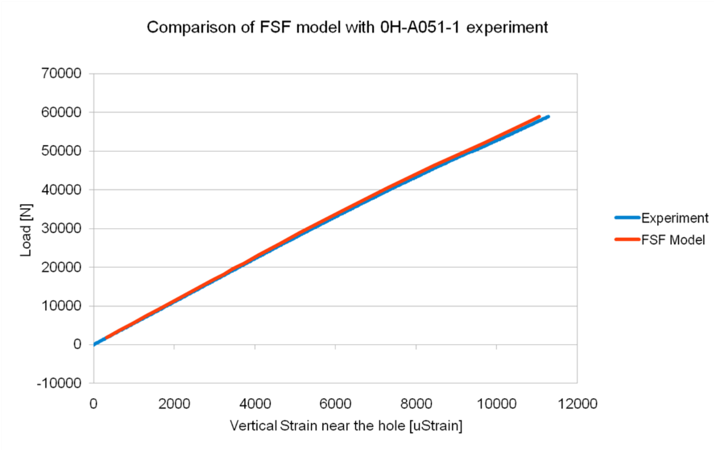


**FIGURE 6**: OPEN HOLE SPECIMEN LOAD VS. STRAIN FOR THE FSF

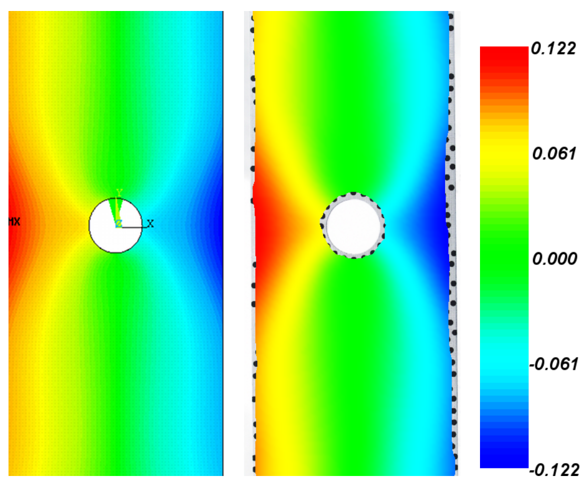


(a) FEA $u_x$ (b) ReMDis 2D $u_x$

**FIGURE 7**: FEA - FULL FIELD MEASUREMENT COMPARISON IN mm

ANSYS SOLID185 element. Indicative views of the meshed geometry are presented in Fig. 4.

For each layer, a transversely isotropic material model was used with the orientation of each 3D layer was modeled using a different ANSYS local coordinate system. The application of the boundary condition was done with the aid of a master node located at the center of the specimen. Although no major difference were observed between linear and non-linear solvers, the analysis presented herein was executed with a non-linear solver and consisted of approximately 300,000 Degrees of Freedom.

First we compare load vs. strain results, Fig. 5, for two different size holes and two tests each. The prediction are based on the SSF.

The differences between prediction and experiment are less than 3% for the high values of the load and and strain ranges.

For higher levels of strain and load some nonlinearity appeared as shown in Fig. 6. The FSF prediction used for this case demonstrate that the prediction is within 1.5% of error at the very high levels of the range.

Next, we present the results from the MRGM measurements along with the corresponding FEA contour plots. The displacement components are shown in Figs. 7 and 8 while the strain components in Figs. 9. In all the figures and all components, the contours are very similar both quantitatively and qualitatively between the ReMDiS-2D results from the experiments and the FEA results. A small difference can be detected for the most cases near the edge of the hole. This can be attributed to the fact that the density of the marks on the specimen is not high enough to represent the more detailed field.

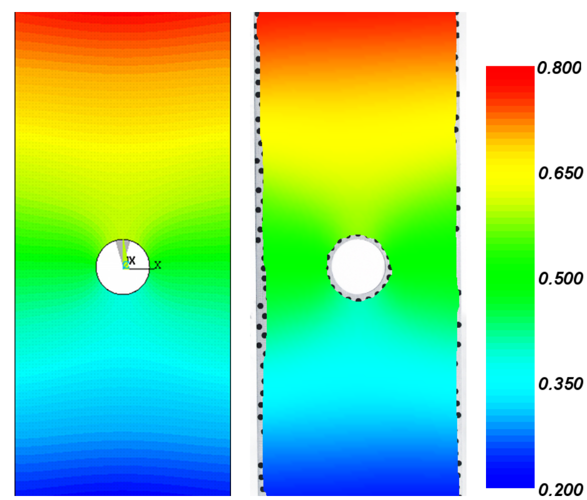


(a) FEA $u_y$ (b) ReMDis 2D $u_y$

**FIGURE 8**: FEA - FULL FIELD MEASUREMENT COMPARISON IN mm

## VALIDATION WITH STIFFENED PANEL SPECIMENS

The third and last validation simulations were performed for specimen manufactured as segments of a stiffened panel under tension. The specimens used for the validation tests were manufactured from the same base material used to construct the characterization specimens but in different layup.

The original stiffened panel and its layup are shown in Fig. 10. Two types of stiffened panel specimens, SP-A and SP-B Figs.

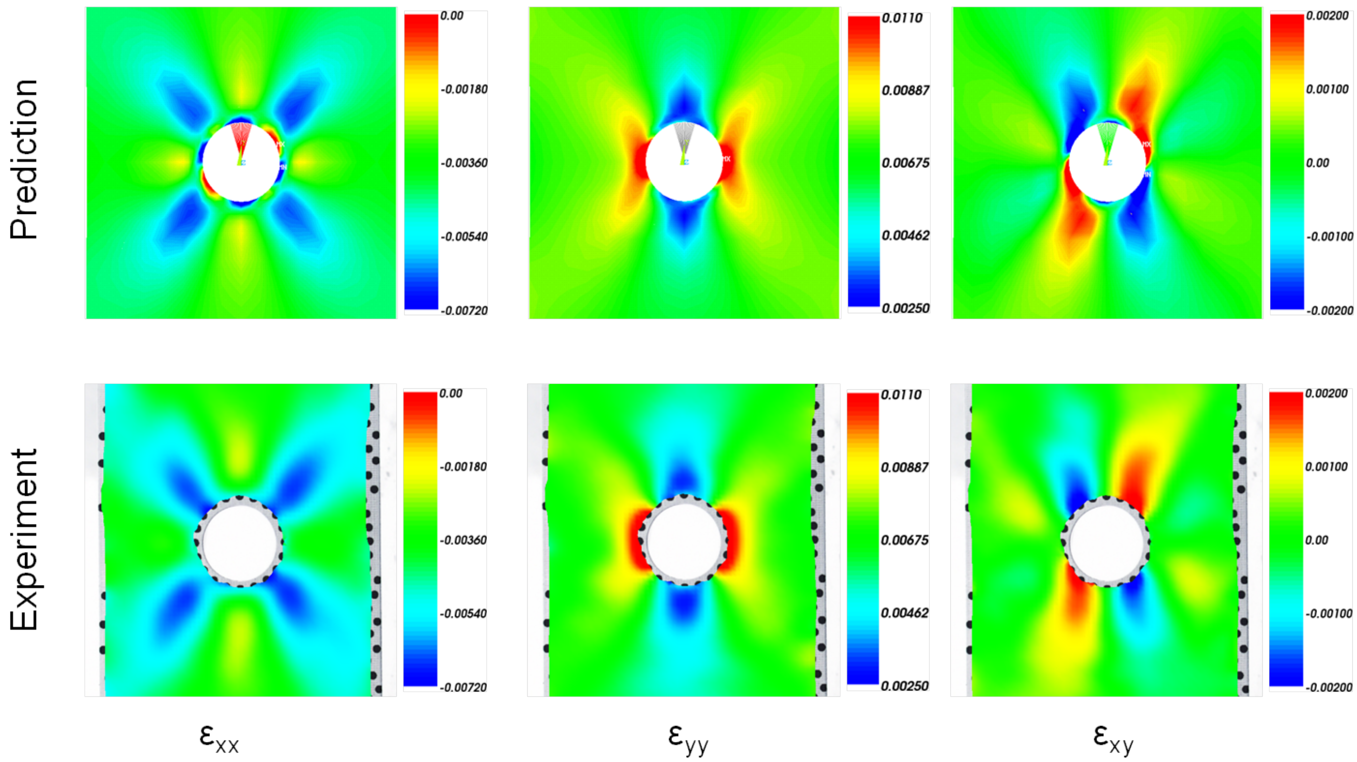


**FIGURE 9**: OPEN HOLE SPECIMEN STRAIN FIELD COMPONENTS FOR THE FSF

•Lay-up regions in skin
(ply 1 at the bottom surface, 0 deg in the stiffener direction):

- S8 $[45/-45/90/0]_S$
- S10 [45/-45/90/0/45/-45/0/90/-45/45]
- S12 $[45/-45/90/0/45/-45]_S$
- U8 [45/-45/90/0/0/90/45/-45]
- U10 [45/-45/90/0/45/-45/0/90/45/-45]
- U12 [45/-45/90/0/45/-45/45/-45/0/90/45/-45]

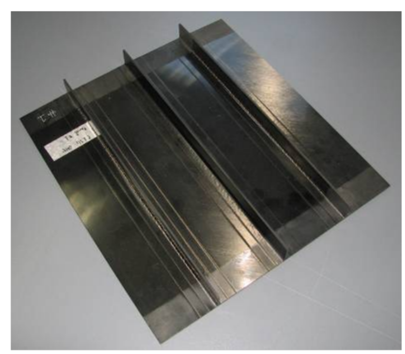

•Lay-up regions in stiffener (0 deg in stiffener direction):

- B16 $[-45/+45/90/0/0/-45/+45/0]_S$

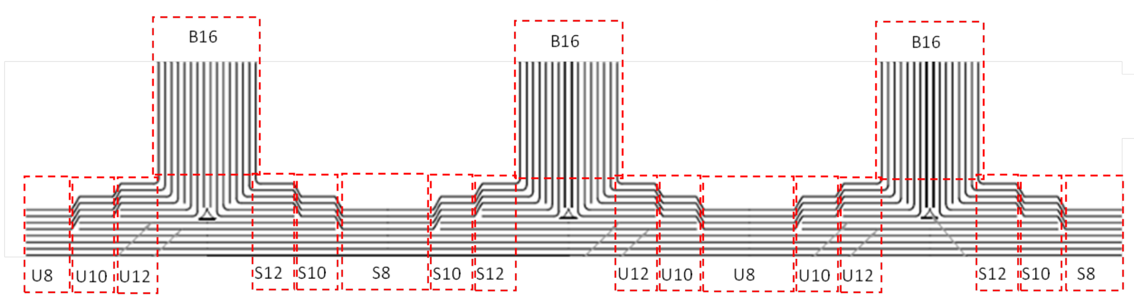


**FIGURE 10**: STIFFENED PANEL AND LAYUP DEFINITION

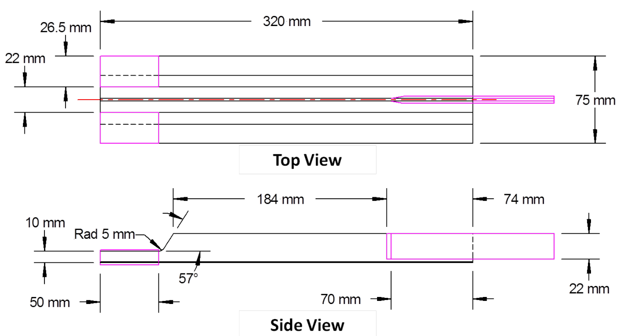


**FIGURE 11**: STIFFENED PANEL SPECIMEN TYPE A

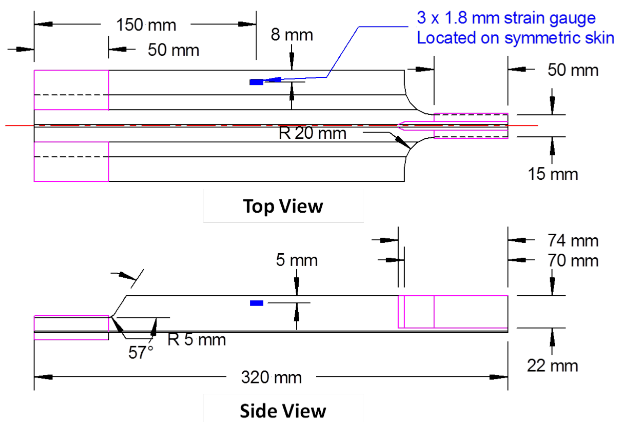


**FIGURE 12**: STIFFENED PANEL SPECIMEN TYPE B

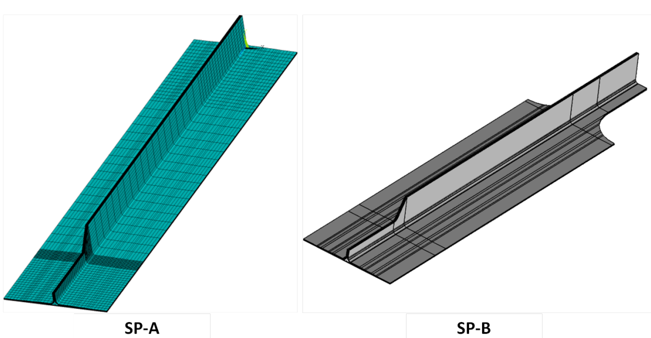


**FIGURE 13**: GEOMETRICAL MODELS OF SP SPECIMENS SP-A AND SP-B

11 and 12 respectively, were cut from the panel element of Fig. 10.

The side of the skin away from the stiffener was marked with white dots in order to use RemDiS-3D during testing for tracking the evolution of the displacement and strain full fields.

On the unmarked side of the specimens, strain-gauges were

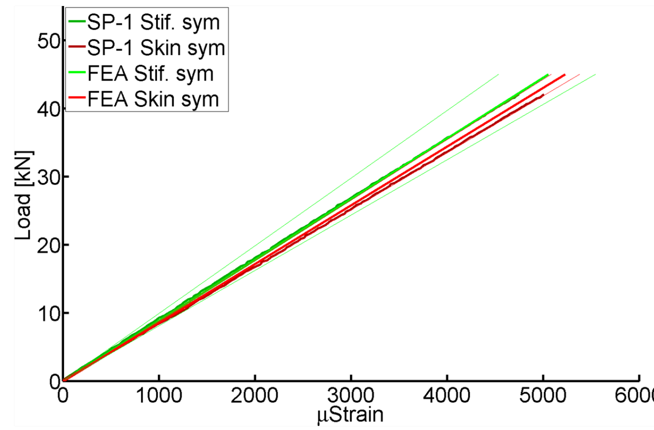


(a) Specimen 1

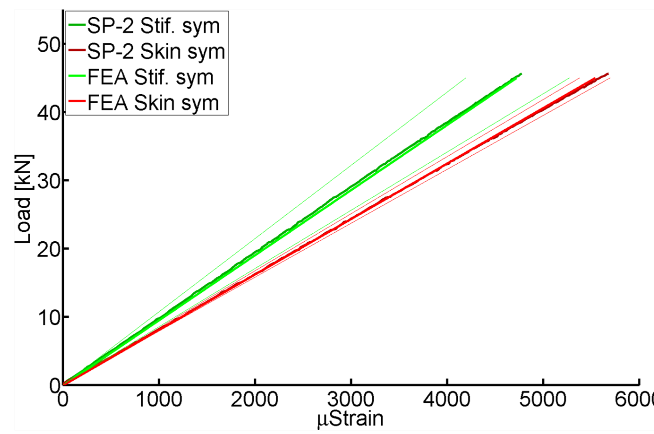


(b) Specimen 2

**FIGURE 14**: LOAD VS. STRAIN FOR STIFFENED PANEL SPECIMENS OF TYPE A IN TENSION

attached, located as shown in Fig. 12.

Figure 13 shows overviews of the geometrical models of SP-A and SP-B made for the FEA. Again the model used the SOLID185 type element in ANSYS.

The specimens were tested in tension at CRC-ACS in Australia. The load vs. strain results are shown in Figs. 14 and 15. The designation "SP-1,2,..." refers to the number identifying which specimen was tested.

We have noticed that the simulation results are very sensitive to the misalignment eccentricity between the grips. For this reason we have generated the bounds of this misalignment for $+/-1mm$ as the thin green and red lines in these figures. All simulation and and experimental results fall well within these misalignment bounds with the exception of the prediction for the skin asymmetric line as shown in Fig. 15(a).

Again the maximum difference between prediction and simulation range between 1.5% and $< 3\%$.

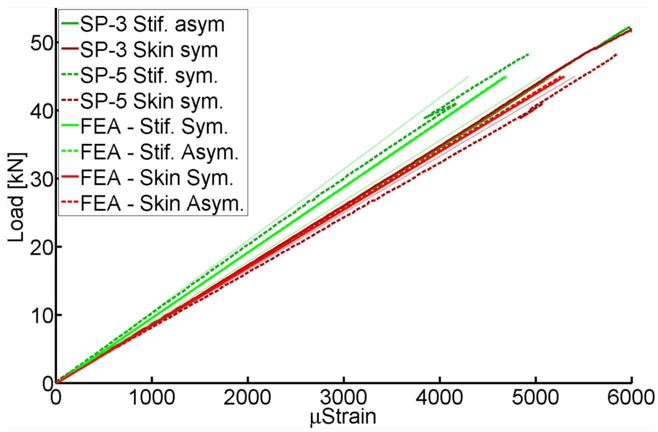


(a) Specimens 3 and 5

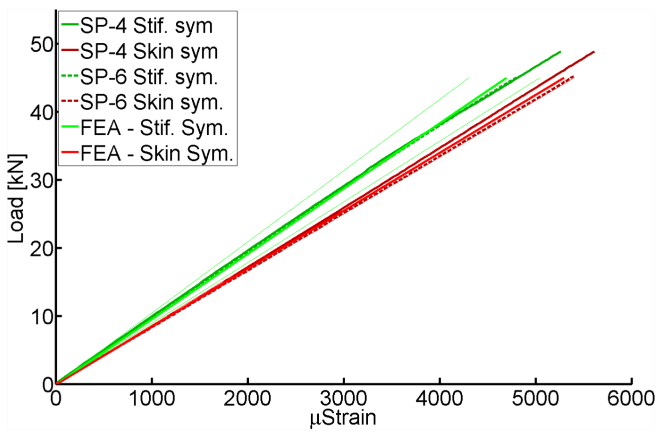


(b) Specimens 4 and 6

**FIGURE 15**: LOAD VS. STRAIN FOR STIFFENED PANEL SPECIMENS OF TYPE B IN TENSION

Finally, Fig. 16 shows a typical comparison between the strain fields measured at the back side of SP-3 (which is of type SP-B) with ReMDiS-3D package [12] next to the FEA prediction for the case of the SSF. The differences again are well within the error of the experimental method. The hot spots near the edges of the grips are artifacts of the absolute boundary conditions applied for simulating the tension of the SP specimens.

It is worthwhile mentioning that the theoretical predictions were conducted blindly relative to the experimental results per the specification of the organization funding our research.

## CONCLUSIONS

In this paper, we have presented a comparison of behavior predictions from FEA models based on the characterized constitutive behavior for both SSF and FSF vs experimental results of actual specimens. This was done for the purpose of validating the methodology of establishing the constitutive behavior of composites by using the data-driven methodology developed by using massive multiaxial tests conducted via the use of the mechatronically automated system developed at NRL that is named NRL66.3.

The coincidence between experiment and prediction for all tests conducted, clearly suggests our characterization methodology is successful in identifying the proper constitutive behavior and the associated material parameters.

This success provides confidence into pursuing our plans for utilizing the energy-based constitutive characterization to formulate failure criteria and address the very important issue of predicting failure for design and maintainability purposes.

## ACKNOWLEDGMENT

This research was partly supported by the US Office of Naval Research (ONR) under NICOP grant N000140-71-05-6-8, and Naval Research Laboratory's (NRL) core funding as well as funding from ONR to NRL. The authors gratefully acknowledge the assistance in experimental testing of Mark McVilley of CRC-ACS and Andrew Litchfield of RMIT University.

## REFERENCES

[1] Michopoulos, J., Hermanson, J., Iliopoulos, A., Lambrakos, S., and Furukawa, T., 2011. "Data-driven design optimization for composite material characterization". *Journal of Computing and Information Science in Engineering,* ***11***(2).

[2] Michopoulos, J., Hermanson, J. C., Iliopoulos, A., Lambrakos, S., and Furukawa, T., 2011. "Overview of constitutive response characterization for composite materials via data-driven design optimization". In Proceedings of the ASME 2011 International Design Engineering Technical Conferences & Computers and Information in Engineering Conference IDETC/CIE, August 29-31, 2011, Washington, DC, USA.

[3] Michopoulos, J., Hermanson, J. C., and Iliopoulos, A., 2012. "First industrial strength multi-axial robotic testing campaign for composite material characterization". In Proceedings of the ASME 2012 International Design Engineering Technical Conferences & Computers and Information in Engineering Conference IDETC/CIE, August 12-15, 2012, Chicago, IL, USA. Submitted.

[4] ANSYS® mechanical, release 12.0.

[5] Michopoulos, J. G., Iliopoulos, A. P., and Furukawa, T., 2009. "Accuracy of inverse composite laminate characterization via the mesh free random grid method". *ASME Conference Proceedings,* ***2009***(48999), pp. 367–374.

[6] Andrianopoulos, N. P., and Iliopoulos, A. P., 2006. "Displacements measurement in irregularly bounded plates us-

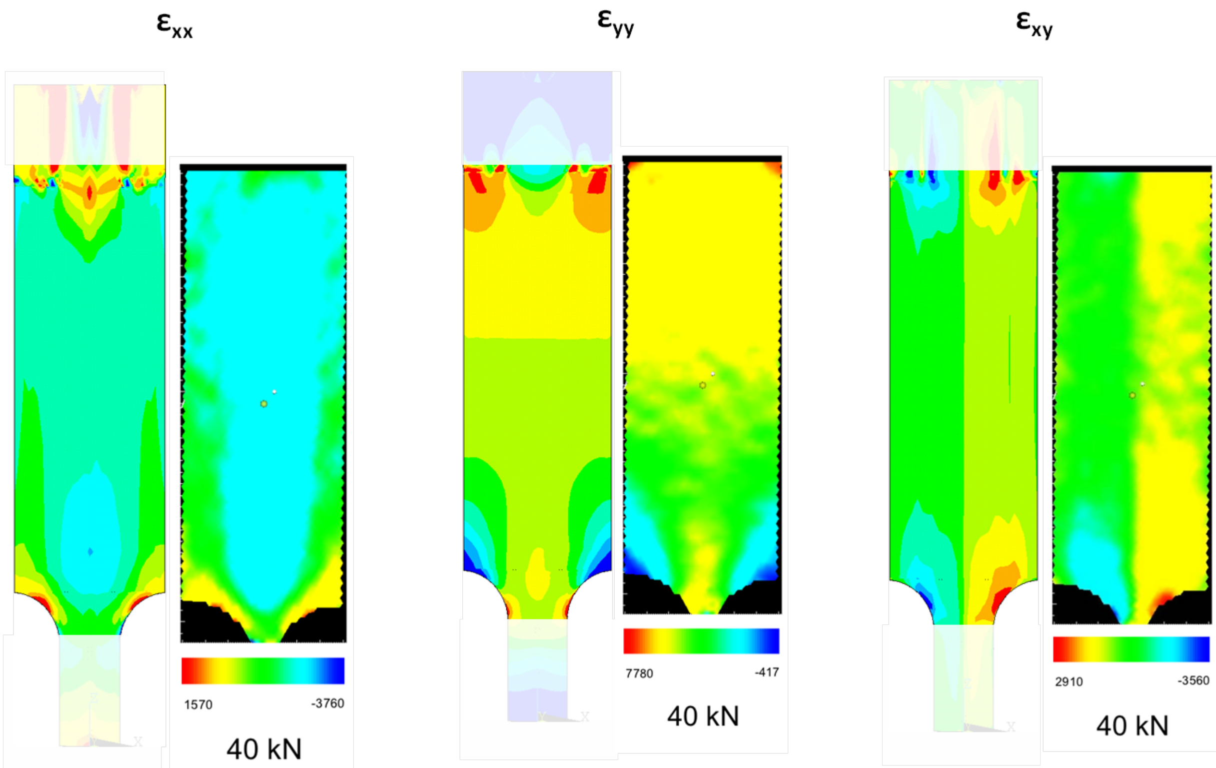


**FIGURE 16**: EXPERIMENTAL VS. PREDICTED STRAIN FIELDS FOR SP-3

ing mesh free methods". In Proc. 16th European Conference of Fracture, Alexandroupolis, Greece, July 3–7.

[7] Iliopoulos, A. P., Michopoulos, J. G., and Andrianopoulos, N. P., 2008. "Performance sensitivity analysis of the Mesh-Free Random Grid method for whole field strain measurements". *ASME Conference Proceedings,* ***2008***(43277), pp. 545–555.

[8] Iliopoulos, A. P., Michopoulos, J. G., and Andrianopoulos, N. P., 2010. "Performance analysis of the Mesh-Free Random Grid Method for full-field synthetic strain measurements". *Strain*, p. In Print.

[9] Iliopoulos, A., and Michopoulos, J., 27–31 Jul 2009. "Sensitivity analysis of the mesh-free random grid method for measuring deformation fields on composites". In Proceedings of the 17th International Conference on Composite Materials, ICCM-17, Edinburgh, The British Composites Society: Edinburgh International Convention Centre (EICC), Edinburgh, UK, 2009.

[10] Iliopoulos, A. P., and Michopoulos, J. G., 2009. "Effects of anisotropy on the performance sensitivity of the Mesh-Free random grid method for whole field strain measurement". *ASME Conference Proceedings,* ***2009***(48999), Jan., pp. 65–74.

[11] Michopoulos, J. G., and Iliopoulos, A. P., 2009. "A computational workbench for remote full field 2d displacement and strain measurements". *ASME Conference Proceedings,* ***2009***(48999), pp. 55–63.

[12] Michopoulos, J., and Iliopoulos, A., 2011. "A computational workbench for remote full field 3d displacement and strain measurements". In Proceedings of the ASME 2011 International Design Engineering Technical Conferences & Computers and Information in Engineering Conference IDETC/CIE, August 29-31, 2011, Washington, DC, USA.